Deflection and stress behaviour of multi-walled carbon nanotube reinforced laminated composite beams

Achchhe Lal[*] and Kanif Markad[a]

Department of Mechanical Engineering, SVNIT Surat-395007, India

Abstract.   The paper presents the thermo-mechanically induced non-linear response of multiwall carbon nanotube reinforced laminated composite beam (MWCNTRCB) supported by elastic foundation using higher order shear deformation theory and von-Karman non-linear kinematics. The elastic properties of MWCNT reinforced composites are evaluated using Halpin–Tsai model by considering MWCNT reinforced polymer matrix as new matrix by dispersing in it and then reinforced with E-glass fiber in an orthotropic manner. The laminated beam is supported by Pasternak elastic foundation with Winkler cubic nonlinearity. A generalized static analysis is formulated using finite element method (FEM) through principle of minimum potential energy approach.

Keywords: FEM; Multiwall carbon nanotube; laminated composite beam; elastic foundation

1. Introduction

The use of novel and advanced composites as an engineering materials has been increased in recent years. These advanced composite material given more prominence for the use of carbon nanotube (CNT) reinforcement using partially or fully because of their outstanding mechanical properties. These properties thus need to be utilized and vary in order to implement materials for high performance structural composites with substantial application potentials. The performance of multiphase composite depends upon the elastic and mechanical properties of fiber and matrix both. The elastic and mechanical properties of the matrix can be increased by inserting carbon nanotube as single wall or multiwall and then conventional fibers are added to the CNT reinforced matrix to make it more superior properties for aerospace and other allied applications. Beam structures are often supported by elastic foundations and occupy an important place for solving many realistic problems related to the structural mechanics such as bridge structures, suspension systems in automobiles, launching pad of missiles, tops etc. To represent the actual behavior of foundation, Pasternak foundation consist of spring and shear layers has been proved as most successful and very convenient for design perspective.

The realistic modeling and analysis of elastic foundation and its effect on structural performance is one of the areas of the research. During applications, in addition to mechanical loading, structures are often subjected to thermal loading. This thermal loading reduces the strength and ultimately lowers the structural performance. Therefore, cautious evaluation of thermal loading is required for optimum performance.

Many researchers have been given more attention on the mechanical properties of carbon nanotube-reinforced composites. In this direction, Thostenson *et al.* (2001) proposed that CNTs are dispersed in the matrix to improve the mechanical and elastic properties and then fibers are added into CNT dispersed matrix, so that multi-phase composite material possess outstanding thermo-electro-mechanical properties can be achieved. Wan *et al.* 2005 investigated the effects of length of CNT and CNT matrix interphase on the elastic properties of CNTRC using finite element. The results indicate the fiber length is critical both to the load transfer efficiency and effective moduli of the composite. Han *et al.* (2007) employed the molecular dynamics (MD) and energy minimization simulation methods to investigate the elastic moduli of the polymer/CNT composite systems. The simulation results suggested the possibility of using CNTs to mechanically reinforce both of these two polymer matrices especially in the tube longitudinal direction. Kapania *et al.* (1989) reviewed the developments in laminated plate and beam analysis with an emphasis on shear effects and buckling. To analyze thin and thick laminated beams and plates suggested the development in finite elements. Finally, a review of the various studies on the delamination buckling and growth in beams and plates is given. Wuite *et al.* (2005) examined the deflection and stress behaviors of nano composite beams by using micromechanics relations to determine the elastic constants in terms of nanotube volume fraction. Classical laminate theory is used to analyze the performance of a CNTRC beam.

It was observed that a small percentage of nanotube reinforcement leads to significant improvements in beam

∗Corresponding author, Assistant Professor
  E-mail: achchhelal@med.svnit.ac.in,
        lalachchhe@yahoo.co.in
[a]Research Scholar
  E-mail: kmarkad13@gmail.com

stiffness. It was shown that stacking sequence and the nanotube diameter are important parameters for reducing the maximum deflection. So many researchers worked on CNT as reinforcement, and used different models to find their equivalent properties. Some of these are, Chakraborty *et al*. (200) developed the exact shear deformable finite element for analysis of FGM. The developed element is based on FSDT, and it is used to study static analysis of single material and bimaterial beams fused with FGM layer. Zhang (2017) evaluated the mechanical behavior of laminated composite with SWCNTs as a reinforcement plate analyzed for sudden transverse load by first order shear deformation theory (FSDT), element-free IMLS-Ritz method utilized. The Mori-Tanaka method is used to find material properties of CNTRC. The results concluded that when the plate is having FG-X CNT the stiffness is the strongest. Syed *et al*. (2017) performed the static analysis of fiber reinforced composite (FRC) shell panel under different loading and boundary conditions (BC) using FSDT based on FEM. It is observed that Centre deflection increase with increase of curvature ratio and deflection of cross-ply plate is higher than angle ply panels. In the same direction (Kerur 2013, Capozucca 2002, Deng 2007, Colombi 2005, Thuc 2012) were performed the static and dynamic either linear or nonlinear analysis of CFRP plate and beams. Along with static, dynamic response, many researchers worked with the effect of foundation and hygro-thermal environment. Virendra *et al*. (2014) examined the second order statistics in terms mean and coefficient of variation (COV) of nonlinear transverse central deflection response of ESSWCNTRCB composed of uniformly distributed and functionally graded reinforcements in thermal environments with uncertain system properties. The transverse central deflection of CNRTC beam is maximum at the center of the beam when the beam is subjected uniform pressure and decreases by increasing the volume fraction index and foundation parameters. Song *et al*. (2006) applied the asymptotic expansion homogenization (AEH) method for elastic properties of the CNT reinforced nano composites. To implement AEH, a control volume finite element method is employed and observed that the homogenized elasticity tensor shows good agreement with the obtained results from Halpin-Tsai equation and is linearly increased with respect to the CNT volume fraction. As the (l/d) of CNT increases, the AEH provides higher axial tensile modulus than the analytic model and the moduli obtained by both methods approach the upper limiting value obtained by the rule of mixture. Bhardwaj *et al*. (2013) presented the effects of variation in the CNT percentage and its aspect ratio on the non-linear flexural and dynamic response of the laminated composite plates using finite double Chebyshev polynomials by utilizing Halpin-Tsai model. SWCNT reinforcement produces more pronounced effect on the static and dynamic response of the plate in comparison on MWCNT on transverse central deflection.

The study of linear and non-linear bending analysis of CNTRC beams subjected to various transverse and in plane load is important due to fact that in practical situations large deformation is expected to occur for different engineering applications from many point of view. Also, modeling and determination of the elastic foundation to obtain accurate response of overall structure is also a matter of concern in the practice. In this direction, Singh *et al*. (2008) presented an investigation of the stochastic nonlinear bending response of a laminated composite plate resting on a two parameter Pasternak elastic foundation with Winkler cubic nonlinearity through uncertain system properties subjected to transverse distributed static load. The COV of the static deflection shows different sensitivity to different system properties. The sensitivity changes with the lay-up sequence, the plate side to thickness ratio, the plate aspect ratio, the boundary conditions and the elastic foundation models. Ying *et al*. (2008) examined the free vibration and bending of functionally graded material beams which is resting on a Winkler-Pasternak elastic foundation using two-dimensional theory of elasticity. The comparisons for homogeneous beams resting on elastic foundations and functionally graded material beams without elastic foundations are performed to illustrate the proficiency of the present method. Shen (2009) suggested for the first time that the nonlinear bending behaviour of CNTRC plates can be considerably improved through the use of a functionally graded distribution of CNTs in the matrix. Functionally graded materials (FGMs) are inhomogeneous composites characterized by smooth and continuous variations in both compositional profile and material properties. Lal *et al*. (2007) studied the effect of randomness in material properties and foundation stiffness parameters on the free vibration response of laminated composite plate resting on an elastic foundation using a C^0 finite element method for an eigenvalue problem and higher order shear deformation theory for model the displacement field. Shi *et al*. (1998) investigated the bending strains effect of the interpolation order with HSDT and showed the accurate third-order composite beam element. This shows that in the finite element modeling of composite beams with HSDT the approximation order of the element bending strain in terms of the deflection and shear deformation can be one order higher than that in terms of the rotation under the same number of nodal variables. Shen *et al*. (2011) studied the non-linear bending, vibration and post-buckling using Euler Bernoulli beam resting on a two-parameter elastic foundation. Result shows that there is a good effect on the nonlinear bending and vibration behaviors of Euler Bernoulli beams with and without elastic foundations. Also, Vahid Tahouneh (2017a, b, 2018) utilized the MWCNTRC core in a sectorial and annular sandwich plates also for curve panel of FG-MWCNTs, for the free vibration characteristic based on the 3D elasticity theory with and without Pasternak foundation. The material properties were found by the modified Halpin-Tsai equation. Free vibrational analysis of thick FG sandwich plates has been done under different boundary conditions and validated the 2D generalized differential quadrature /numerical method to analyses the laminated sectorial sandwich plate. Also the effect of material parameter, geometrical parameters and 2-paramter elastic foundation checked on frequency parameters of the sandwich plate. Results defined the effect of different volume fraction of MWCNT on vibration behaviour of functionally graded multi walled carbon

nanotube curved thick panels.

Most studies on CNTRCs have focused on material properties of functionally graded composite material and their analysis. The aim of these studies is to develop the new class of materials. Some of the investigations show that the addition of small amounts of CNT can considerably improve the mechanical, thermal and electrical properties of polymeric composites (Fidelus 2005, Bonnet 2007, Han 2007, Zhu 2007). Even though, these studies are quite useful in establishing the stress-strain behavior of the nano-composites. As a result, there is a need to observe the global response of CNTRCs in an actual structural element. Wuite *et al.* (2005) examined the deflection and stress of nano composite reinforced beams using a multi-scale analysis. Kishan *et al.* (2017) developed a higher-order shear deformation theory to study the bending behavior of simply supported CNT reinforced Metal Matrix composite plate without any transverse shear stress on top and bottom surfaces of plate and concluded that the bending responses of functionally graded material plates mainly depends on the type of CNT distribution and volume fraction. Yas *et al.* (2012) studied the vibrational properties of functionally graded nano composite beams reinforced by randomly oriented straight SWCNTs under the actions of moving load. The Eshelby-Mori-Tanaka approach based on an equivalent fiber is used to investigate the material properties of the beam. It is observed that, various material distributions, carbon nanotube orientations, velocity of the moving load, shear deformation, slenderness ratios and boundary conditions play very important role on the dynamic behaviour of the beam. Kumar *et al.* (2017) identified the static and dynamic behavior of functionally graded polymer composite plates reinforced by MWCNT using noval layer-wise formulation concept. Halpin Tsai model is used to predict elastic property of nano composite materials. The result shows that there is a significant effect of nanotube weight fraction and length and diameter (l/d) ratio of MWCNT on natural frequencies, critical buckling and bending of the nano composite plate. Yas *et al.* (2012) studied the free vibrations and buckling of nano composite beams reinforced by SWCNT resting on an elastic foundation have been studied using Timoshenko beam theory. The material properties have been estimated though the rule of mixture. The numerical results reveal that the distribution of CNT, foundation stiffness and volume fraction of CNT have significant effects on the natural frequencies and critical buckling load of the CNTRC beams. Pradhan *et al.* (2011) employed Eringen equations to find Non-local elasticity and buckling analysis of SWCNT with elastic foundation and temperature effect. The effect of the Winkler modulus, beam size, non-local parameter and temperature change of SWCNT's on non-local critical buckling load are investigated and discussed. Shen (2000) observed that by CNTRC beam with intermediate CNT volume fraction does not necessarily have intermediate nonlinear frequencies, buckling temperatures and thermal post buckling strengths using semi analytical approach through HSDT. Sina *et al.* (2009) developed a new beam theory which is different from the FSDT beam theory is used for the analysis of free vibration

of FGM beams. This shows that the new theory is more accurate in natural frequency from the traditional FSDT and the mode shapes of the two methods are coincidental.

Carbon nanotube reinforced composite layers are made from the uniformly dispersed CNT into the conventional matrix along the thickness direction. By utilizing several micromechanical models like the Mori-Tanaka model and the Voigt model as the rule of the mixture, there will be prediction of the effective material properties of CNTRCs. In this paper, the Halpin-Tsai approach is utilized to predict the global material properties and responses of the CNTRC structures.

Relatively very little work is available related to thermo mechanical induced nonlinear flexural analysis of elastically supported multiwall carbon nanotube reinforced multiphase composite beam to the best of author's knowledge. The literature reveals that most of the work are related to mechanical properties evaluation of fully CNT reinforced polymer composites without considering thermal effect. Very limited attention is paid to study of MWCNT reinforced with polymer matrix and assuming as new matrix and then reinforced with conventional E-glass fiber in an orthotropic manner to increase transverse resistance. The effect of load parameters, CNT volume fraction, number of single wall CNTs, thickness and aspect ratio of CNTs, support conditions, beam slenderness and thickness ratios, temperature change and foundation parameters and lamination scheme on the nonlinear flexural and stresses are studied.

2. Formulations

2.1 Geometry configuration of elastically supported beam

A elastically supported multiwall carbon reinforced composite beam (ESMWCNTRCB) supported by elastic foundation consist of nonlinear spring and shear foundation with beam length (*a*) and thickness (*h*) in one dimensional (1-D) plane along its co-ordinate definition and material directions of lamina in (*x*, *z*) coordinate system is shown in Fig. 1.
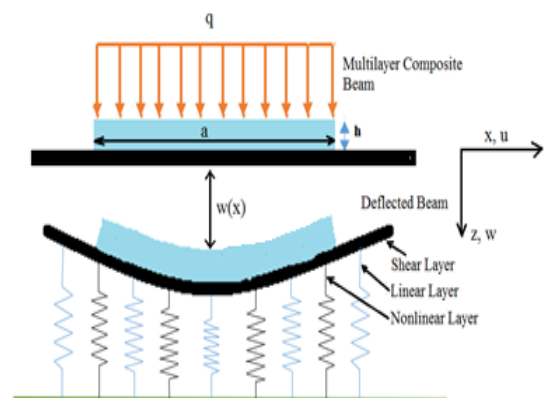

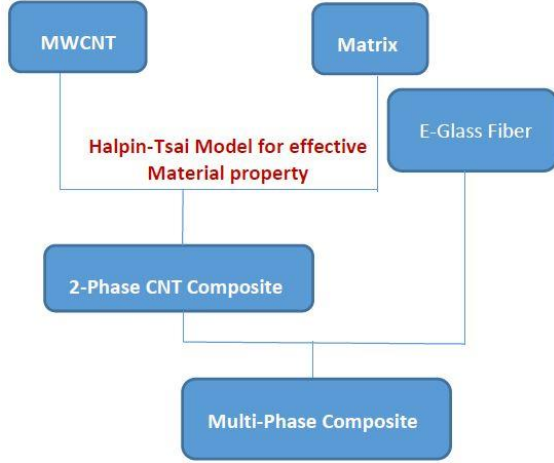Fig. 1 Geometry of CNTRC beam resting on nonlinear elastic foundation

Fig. 2 Flow chart for the preparation of SWCNT and MWCNT reinforced composite

The bonding between the SWCNT/MWCNT and matrix is assumed to be perfect and strain experience by the matrix and MWCNT are also equal. MWCNTRCB is attached to supporting foundation excluding any separation takes place in the process of deformation. The interaction between the beam and the supporting foundation follows the one parameters Pasternak model with Winkler cubic nonlinearity (Sina 2009). By the supporting foundation reaction forces are exerted and magnitude of that reaction forces per unit area will be as (Caudhari *et al*. 2014, Shegokar *et al*. 2013)

$$p = K_1 w + K_3 w^3 - K_2 \frac{\partial^2 w}{\partial x^2} \qquad (1)$$

where w is the transverse displacement of the MWCNTRCB. The parameters used in the supporting foundation K_1, K_2 and K_3 are linear normal, shear and nonlinear normal foundation stiffness's, respectively. The Eq. (1) can be reduced as Winkler type by neglecting $K_2=0$.

2.2 Material properties of carbon nanotube reinforced composite by Halpin-Tsai model

The elastic properties of CNT reinforced multi-scale composites are evaluated using Halpin-Tsai Model through micromechanical approach. Fig. 2 shows the layout for evaluating the elastic properties of the CNT reinforced multi-phase composites (Bhardwaj *et al* 2013).

The Halpin-Tsai approach is used to find the elastic properties of multi wall carbon nanotube composites (MWCNTRC) by varying both the volume fraction of CNT. The tensile modulus of carbon nanocomposite can be expressed as (Bhardwaj *et al* 2013), Kumar *et al*. 2017)

$$E_m = \left\{ \left(\frac{3}{8}\right) E_L + \left(\frac{5}{8}\right) E_T \right\} \qquad (2)$$

Where

$$E_L = \left[\frac{1 + \xi_L \eta_L V_{mw}}{1 - \eta_L V_{mw}} \right] E_m; \qquad E_T = \left[\frac{1 + \xi_T \eta_T V_{mw}}{1 - \eta_T V_{mw}} \right] E_m;$$

With

$$\eta_L = \frac{(E_{mw}/E_m)-1}{(E_{mw}/E_m)+2(L/t)}; \quad \eta_T = \frac{(E_{mw}/E_m)-1}{(E_{mw}/E_m)+2};$$

Where E_m and L are the Young's modulus of epoxy and length of MWCNTs. The thickness of CNT can be written as (Kumar *et al*. 2017)

$$t = \left(\frac{D_{mo} - D_{mi}}{2} \right) \qquad (3)$$

Where, $D_{mo} = D_{so} + 2(N_w - 1)h_{in}$; $D_{mi} = D_{si}$ and $D_{so} = D_{cnt} + t_{cnt}$; $D_{si} = D_{cnt} - t_{cnt}$;
With

$$D_{cnt} = \frac{\sqrt{3(m^2 + n^2 + mn)}}{\pi} a_{c-c}; \qquad (4)$$

Where (m, n) indicate the chiral vector of nanotube as (5, 5), (10, 10), (20, 20) and a_{c-c} is the carbon-carbon bond length of SWCNT.

The effective elastic modulus of MWCNT (Y_i^{mw}) is written as (Kumar and Srinivas 2017)

$$Y_i^{mw} = \frac{N_w t_{cnt} Y_i^{cnt}}{(N_w - 1)h_{in} + t_{cnt}} \qquad (5)$$

Where Y_i^{cnt} is the effective elastic properties in the form of Young's moduli, shear modulus, Poisson's ratio and density of SWCNTs, t_{cnt} is the wall thickness of single wall CNTs. N_w and h_{in} are number of CNTs walls and inter-wall spacing in MWCNTs chosen as $1.5t_{cnt}$. The thickness of CNTs is assumed as 0.335 nm (unless otherwise mentioned). However, h_{in} for MWCNTs varies from 0.27 to 0.42 nm.

It is assumed that the addition of number of walls in MWCNTs configuration do not change Poisson's ratio ($v_{mw}=v_{cnt}$) and density ($\rho_{mw}=\rho_{cnt}$) respectively.

The CNT reinforced matrix (E_m) is further reinforced with E-Glass fiber in an orthotropic manner. Micromechanics approach is used to determine the elastic properties of the composites (Deng *et al*. 2007)

The longitudinal modulus of composite can be expressed as (Bhardwaj *et al*. 2013)

$$E_1 = E_f V_f + E_m V_m \qquad (6)$$

The transverse modulus of composite is expressed by

$$E_2 = \left[\frac{1 + \xi_T \eta_T V_{mw}}{1 - \eta_T V_{mw}} \right] E_m; \text{ where } \eta_T = \frac{(E_f/E_m)-1}{(E_f/E_m)+2}; \qquad (7)$$

The in plane shear modulus (G_{12}) is expressed by using the following relationship

$$G_{12} = \left[\frac{1 + \xi_T \eta_T V_{mw}}{1 - \eta_T V_{mw}} \right] G_m; \text{ where } \eta_T = \frac{(G_f/G_m)-1}{(G_f/G_m)+1} \qquad (8)$$

The Poisson's ratio of composite can be expressed as

$$v_{12} = v_f V_f + v_m V_m \qquad (9)$$

Similarly, the effective thermal expansion coefficients in the longitudinal and transverse directions (α_{11}, α_{22}) can be expressed by the Shapery model (Shen 2009)

$$\alpha_{11} = \frac{V_{cn}E_{11}^{cn}\alpha_{11}^{cn} + V_m E^m \alpha^m}{V_{cn}E_{11}^{cn} + V_m E^m} \tag{10}$$

$$\alpha_{22} = \left(1 + v_{12}^{cn}\right)V_{cn}\alpha_{22}^{cn} + \left(1 + v^m\right)V_m\alpha^m - v_{12}\alpha_{11} \tag{11}$$

It is assumed that the material properties of CNTs and matrix are the functions of temperature, so that the effective material properties of CNTRCs, like Young's modulus, shear modulus and thermal expansion coefficients, are also functions of temperature T.

2.3 Material properties of carbon nanotube reinforced composite by Mori Tanaka model

The composite considered here is a three-phase material, with fibers and matrix with MWCNT as its constituents According to the Mori-Tanaka theory and Benveniste's reformulation (Liu and Huang 2014), the relationship between strains and stresses for the matrix and fiber defined as

$$\begin{aligned} \left\{\sigma_i^{\,m}\right\} &= [A_{ij}]\left\{\sigma_j^{\,f}\right\} \\ \left\{\varepsilon_i^{\,f}\right\} &= [T_{ij}]\left\{\varepsilon_j^{\,m}\right\} \end{aligned} \tag{12}$$

Eshelby's tensor is $[T_{ij}]$, and it is calculated as

$$\left[T_{ij}\right] = \left[[I_{ij}] + [L_{ik}][S_{kp}{}^m]\left([C_{pj}{}^f] - [C_{pj}{}^m]\right)\right]^{-1} \tag{13}$$

$[S_{ij}]$, $[C_{ij}]$ are the compliance and stiffness tensors of a material. $[L_{ij}]$ higher order Eshelby's tensor and $[I_{ij}]$ is a second order unit tenor.

Through a Mori-Tanaka's tensor, one can find the relationship between the $[A_{ij}]$ and $[T_{ij}]$

$$\left[A_{ij}\right] = \left[C_{ik}^m\right]\left[T_{KP}\right]^{-1}\left[S_{PJ}^F\right] = \left[C_{ik}^m\right]\left[[Ikq] + [Lkl][S_{lp}^m]\left([C_{pq}^f] - [C_{pq}^m]\right)\right]\left[S_{qj}^f\right] \tag{14}$$

Here the non-zero elements from the matrix are calculated as

$$A_{11} = \frac{E^m}{E_{11}^f}\left[1 + \frac{v^m\left(v^m - v_{12}^f\right)}{\left(1 + v^m\right)\left(1 - v^m\right)}\right]$$

$$A_{12} = \frac{E^m}{E_{11}^f}\left[\frac{v^m\left(1 - v_{23}^f\right)}{2\left(1 + v^m\right)\left(1 - v^m\right)}\right] - \frac{E^m}{E_{11}^f}\frac{v_{12}^f}{\left(1 + v^m\right)\left(1 - v^m\right)} + \frac{v^m}{2\left(1 - v^m\right)} = A_{13}$$

$$A_{22} = \frac{E^m}{E_{11}^f}\left[\frac{v_{23}^f - 3}{8\left(1 + v^m\right)\left(-1 + v^m\right)}\right] - \frac{E^m}{E_{11}^f}\frac{v_{12}^f v^m}{2\left(1 + v^m\right)\left(-1 + v^m\right)} + \frac{\left(v^m + 1\right)\left(4v^m - 5\right)}{8\left(1 + v^m\right)\left(-1 + v^m\right)} = A_{33}$$

$$A_{21} = \frac{E^m}{E_{11}^f}\left[\frac{\left(v^m - v_{12}^f\right)}{2\left(1 + v^m\right)\left(1 - v^m\right)}\right] = A_{31}$$

$$A_{32} = \frac{E^m}{E_{11}^f}\left[\frac{3v_{23}^f - 1}{8\left(1 + v^m\right)\left(-1 + v^m\right)}\right] + \frac{E^m}{E_{11}^f}\frac{v_{12}^f v^m}{2\left(1 + v^m\right)\left(-1 + v^m\right)} + \frac{\left(v^m + 1\right)\left(1 - 4v^m\right)}{8\left(1 + v^m\right)\left(-1 + v^m\right)} = A_{23}$$

$$A_{44} = \frac{G^m}{G_{23}^f}\frac{1}{4\left(1 - v^m\right)} + \frac{\left(3 - 4v^m\right)}{4\left(1 - v^m\right)}$$

$$A_{55} = \frac{G^m + G_{12}^f}{2G_{12}^f} = A_{66}$$

The effective compliance tensor using the Mori-Tanaka's tensor for composite obtained as (Liu and Huang 2014)

$$\left[S_{ij}\right] = \left(V_f\left[S_{ik}^f\right] + V_m\left[S_{ip}^m\right]\left[A_{pk}\right]\right)\left(V_f\left[I_{kj}\right] + V_m\left[A_{kj}\right]\right)^{-1} \tag{15}$$

Volume fraction of matrix and fiber are defined by Vm and V_f respectively, and effective elastic moduli are determined as follows

$$E_{11} = \frac{(V_f + V_m a_{11})(V_f + V_m a_{22}) - A_{12}A_{21}V_m^2}{(V_f + V_m A_{22})(V_f S_{11}^f + V_m A_{11}S_{11}^m) + V_f V_m\left(S_{12}^m - S_{12}^f\right)A_{21} - A_{12}A_{21}V_m^2 S_{11}^m} \tag{16a}$$

$$E_{22} = \frac{(V_f + V_m A_{11})(V_f + V_m A_{22}) - A_{12}A_{21}V_m^2}{(V_f + V_m A_{11})(V_f S_{22}^f + V_m A_{22}S_{22}^m) + V_f V_m\left(S_{21}^m - S_{21}^f\right)A_{12} - A_{12}A_{21}V_m^2 S_{22}^m} \tag{16b}$$

$$G_{12} = \frac{(V_f + V_m A_{66})G_{12}^f G^m}{V_f G^m + V_m A_{66}G_{12}^f} \tag{16c}$$

$$v_{12} = -\frac{(V_f + V_m A_{11})(V_f S_{12}^f + V_m A_{22}S_{12}^m) + V_f V_m(S_{11}^m - S_{11}^f)A_{12} - A_{12}A_{21}V_m^2 S_{12}^m}{(V_f + V_m A_{22})(V_f S_{11}^f + V_m A_{11}S_{11}^m) + V_f V_m\left(S_{12}^m - S_{12}^f\right)A_{21} - A_{12}A_{21}V_m^2 S_{11}^m}$$

$$v_{12}^* = -\frac{(V_f + V_m A_{22})(V_f S_{12}^f + V_m A_{11}S_{12}^m) + V_f V_m(S_{11}^m - S_{22}^f)A_{21} - A_{12}A_{21}V_m^2 S_{12}^m}{(V_f + V_m A_{22})(V_f S_{11}^f + V_m A_{11}S_{11}^m) + V_f V_m\left(S_{12}^m - S_{12}^f\right)A_{21} - A_{12}A_{21}V_m^2 S_{11}^m} \tag{16d}$$

2.4 Displacement field model

For an arbitrary CNTRC beam, the components of displacement field model can de expressed as the modified displacement field components along x and z directions of an arbitrary point within the beam based on the HSDT using C^0 continuity in order to reduce computational difficulties can be expressed as (Shegokar and Lal 2013, Reddy 2004)

$$\bar{u}(x,z) = u + f_1(z)\psi_x + f_2(z)\phi_x; \quad \bar{w}(x,z) = w \tag{17}$$

Where u, w, ψ_x and $\phi = \partial w/\partial x$ are the mid-plane axial displacement, transverse displacement, rotation of normal to the mid-plane along *y*-axis and slope along *x*-axis, respectively. The parameter $f_1(z)$ and $f_2(z)$ are expressed as

$$f_1(z) = C_1 z - C_2 z^3, \quad f_2(z) = -C_2 z^3,$$

With

$$C_1 = 1, \quad C_2 = 4/3h^2 \tag{18}$$

To implement this theory, a suitable C^0 continuous isoparametric finite element approach with seven degrees of freedom (DOFs) per node is proposed in order to reduce the computational efforts required in the formulation of element matrices without affecting the solution accuracy.

The displacement vector for the modified C^0 continuous model can be written as

$$\{q\} = \begin{bmatrix} u & w & \phi_x & \psi_x \end{bmatrix}^T \tag{19}$$

2.5 Strain displacement relation

The total strain vector consisting of linear strain (in terms of mid plane deformation, rotation of normal and

higher order terms), non-linear strain (von-Karman type), thermal strains vectors associate with the displacement for MWCNRCB can be expressed as

$$\{\bar{\varepsilon}\} = \{\bar{\varepsilon}^L\} + \{\bar{\varepsilon}^{NL}\} - \{\bar{\varepsilon}^T\} \tag{20}$$

Where $\{\bar{\varepsilon}_L\}$, $\{\bar{\varepsilon}^{NL}\}$ and $\{\bar{\varepsilon}^T\}$ are the linear, non-linear and thermal strain vectors, respectively. From Eq. (20), the linear strain tensor using HSDT can be written as

$$\bar{\varepsilon}^L = [B]\{q\} \tag{21}$$

Where $[B]$ and $\{q\}$ are the geometrical matrix and displacement field vector, respectively. The nonlinear strain vector $\{\bar{\varepsilon}^{NL}\}$ can be written a

$$\bar{\varepsilon}^{NL} = \frac{1}{2}[A_{nl}]\{\phi_{nl}\} \tag{22}$$

Where $\{A_{nl}\} = \frac{1}{2}\left[\frac{\partial w}{\partial x}\right]^T$ and $\{\phi_{nl}\} = \left\{\frac{\partial w}{\partial x}\right\}$

The thermal strain vector $\{\bar{\varepsilon}^T\}$ induced by uniform temperature change can be expressed as

$$\{\bar{\varepsilon}^T\} = \{\alpha_x\}\Delta T \tag{23}$$

Where $\{\alpha_x\}$ is coefficients of thermal expansion along the x direction, and ΔT is the change in temperature in the MWCNTRCB considered as uniform distribution and can be expressed as

$$\Delta T = T - T_0 \tag{24}$$

Where, T is the uniform temperature rise and T_0 is the room temperature and assumed as 300 K.

2.6 Stress-Strain relation

The relation between stress $\{\bar{\sigma}\}$ and strain for the plane-stress case using thermo-elastic constitutive relation can be written as (Shegokar and Lal 2013)

$$\{\bar{\sigma}\} = [Q]\{\bar{\varepsilon}\} \tag{25}$$

$$\begin{Bmatrix} \bar{\sigma}_x \\ \bar{\tau}_{xz} \end{Bmatrix} = \begin{bmatrix} \bar{Q}_{11} & 0 \\ 0 & \bar{Q}_{55} \end{bmatrix} \left\{ \{\bar{\varepsilon}^L\} + \{\bar{\varepsilon}^{NL}\} - \{\bar{\varepsilon}^T\} \right\} \tag{26}$$

Where

$$\bar{Q}_{11} = Q_{11}\cos^4\theta_k + Q_{22}\sin^4\theta_k + 2(Q_{12} + 2Q_{66})\cos^2\theta_k\cos^2\theta_k$$

and

$$\bar{Q}_{55} = Q_{55}\cos^2\theta_k + Q_{44}\sin^2\theta_k \tag{27a}$$

with

$$Q_{11} = \frac{E_1}{1-\nu_{12}\nu_{21}}; \quad Q_{22} = \frac{E_2}{1-\nu_{12}\nu_{21}}; \quad Q_{12} = \frac{\nu_{12}E_2}{1-\nu_{12}\nu_{21}};$$

$$\nu_{21} = \frac{\nu_{12}E_2}{E_1}; \quad Q_{55} = G_{12}; \text{ and } Q_{44} = G_{13} \tag{27b}$$

Here θ_k is represented as fiber orientation. The parameters E_1, E_2, G_{12}, G_{13}, G_{23} and ν_{12} are the longitudinal, transverse and shear modulus, and Poisson's ratio, respectively.

2.7 Strain energy of MWCNTRC beam

The strain energy (Π_1) of the MWCNTRC beam undergoing large deformation can be expressed as

$$\Pi_1 = U_L + U_{NL} \tag{28}$$

The linear stain energy (U_L) of the MWCNTRC beam is written as

$$U_L = \int_A \frac{1}{2}\{\bar{\varepsilon}^L\}^T[Q]\{\bar{\varepsilon}^L\}dA = \int_A \frac{1}{2}\{\bar{\varepsilon}^L\}^T[D]\{\bar{\varepsilon}^L\}dA \tag{29}$$

Where $[D]$ and $\{\bar{\varepsilon}_L\}$ are the elastic stiffness matrix and linear strain vector, respectively.

The nonlinear strain energy (U_{NL}) of the MWCNTRC beam can be rewritten as

$$U_{NL} = \int_A \frac{1}{2}\{\bar{\varepsilon}^L\}^T[D_1]\{\bar{\varepsilon}^{NL}\} + \frac{1}{2}\{\bar{\varepsilon}^{NL}\}^T[D_2]\{\bar{\varepsilon}^L\} + \frac{1}{2}\{\bar{\varepsilon}^{NL}\}^T[D_3]\{\bar{\varepsilon}^{NL}\}dA \tag{30}$$

Where D_1, D_2 and D_3 are the elastic stiffness matrices of the MWCNTRC beam, respectively.

2.8 Strain energy due to foundation

The strain energy (Π_F) due to elastic foundation considering shear deformable layer with Winkler cubic nonlinearity is written as (Shegokar and Lal 2013),

$$\Pi_F = \int_A pwdA \tag{31}$$

The strain energy due to the foundation is expressed as

$$\Pi_F = \frac{1}{2}\int_A \left\{ K_1w^2 + \frac{1}{2}K_3w^4 + K_2\left[(w_{,x})^2\right] \right\}dA \tag{32}$$

Eq. (32) can be further written as matrix form

$$\Pi_F = \frac{1}{2}\int_A \begin{Bmatrix} w \\ w_{,x} \end{Bmatrix}^T \begin{bmatrix} K_1 & 0 \\ 0 & K_2 \end{bmatrix} \begin{Bmatrix} w \\ w_{,x} \end{Bmatrix}dA + \frac{1}{2}\int_A \begin{Bmatrix} w \\ w_{,x} \end{Bmatrix}^T \begin{bmatrix} K_3w^2 & 0 \\ 0 & 0 \end{bmatrix} \begin{Bmatrix} w \\ w_{,x} \end{Bmatrix}dA \tag{33}$$

2.9 Work done due to thermal loadings

The potential of work (Π_2) storage due to thermal loadings can be written as

$$\Pi_2 = \frac{1}{2}\int_A N_0^T(w_{,x})^2 dA \tag{34}$$

The thermal compressive stress/unit length N_0^T can be expressed as

$$N_0^T = \begin{bmatrix} N_x^T & M_x^T & P_x^T \end{bmatrix} \tag{35}$$

The Eq. (34) can be further written as

$$\left(N_x^{\;T}, M_x^{\;T}, P_x^{\;T}\right) = \int\limits_{-h/2}^{h/2} (1,\, z,\, z^3) Q_{11} \alpha \Delta T dz \qquad (36)$$

2.10 Work done due to external applied loading

Work done due external applied uniformly distributed can be written as

$$\Pi_3 = W_q = \int_A q_m\left(x, z\right) w\, dA \qquad (37)$$

Where, $q_m(x,z)$ is the intensity of applied uniformly distributed load. For the uniformly distributed loading $q_m(x,z)$ is written as

$$q_m\left(x, z\right) = \frac{Q E_m I}{a^3} \qquad (38)$$

Where, Q and I are the uniform distributed load parameters and Moment of inertia, respectively.

2.11 Strain energy of the beam element

In the present study, a C^0 one-dimensional Hermitian beam element with 4 DOFs per node is employed. (Fidelus *et al.* 2005) Expressed as this type of beam element geometry and the displacement vector.

$$\{q\} = \sum_{i=1}^{NN} N_i \{q\}_i ; \qquad x = \sum_{i=1}^{NN} N_i x_i ; \qquad (39)$$

Where,
N_i = interpolation function for the ith node
$\{q\}_i$ = the vector of unknown displacements for the ith node
NN = the number of nodes per element
x_i = Cartesian coordinate
The linear interpolation for axial displacement and rotation of normal and Hermite cubic interpolation functions are chosen for transverse displacement and slope. Using finite element model Eq. (39), Eq. (28) can be expressed a

$$\Pi_1 = \sum_{e=1}^{NE} \Pi_a^{(e)} = \sum_{e=1}^{NE} \left(U_L^{(e)} + U_{NL}^{(e)}\right) \qquad (40)$$

Where, NE and (e) denote the number of elements and elemental, respectively.
Eq. (40) can be further expressed as

$$\Pi_1 = \frac{1}{2} \sum_{e=1}^{NE} \left[\{q\}^{T(e)} \left[K_l + K_{nl}\right]^{(e)} \{q\}^{(e)} \right] = \{q\}^T \left[K_l + K_{nl}\right] \{q\} \quad (41)$$

Here $\left[K_{nl}\right] = \frac{1}{2}\left[K_{nl_1}\right] + \left[K_{nl_2}\right] + \frac{1}{2}\left[K_{nl_3}\right]$

Where $[K_l]$, $[K_{nl1}]$, $[K_{nl2}]$, $[K_{nl3}]$ and $\{q\}$ are defined as global linear, nonlinear stiffness matrices and global displacement vector, respectively.

2.12 Foundation analysis

Similarly, using finite element model Eq. (41), Eq. (32)

after assembly procedure can be written as

$$\Pi_F = \sum_{e=1}^{NE} \left(\Pi_F^{(e)}\right) = \left\{q^{(e)}\right\}^T \left[K_{fl} + K_{fnl}\right]^{(e)} \left\{q^{(e)}\right\} = \{q\}^T \left[K_{fl} + K_{fnl}\right] \{q\} \, (42)$$

Where, $[K_{fl}]$ and $[K_{fnl}]$ is the global linear and nonlinear foundation stiffness matrices, respectively.

2.13 Work done due to thermal loadings

Using finite element model Eq. (35) after summing over the entire element can be written as (Fidelus *et al.* 2005)

$$\Pi_2 = \sum_{e=1}^{NE} \Pi_2^{(e)} = \frac{1}{2} \sum_{e=1}^{NE} \{q\}^{T(e)} \lambda \left[K_g\right]^{(e)} \{q\}^{(e)}$$

$$= \frac{1}{2} \lambda \{q\}^T \left[K_g\right] \{q\} \qquad (43)$$

Where, λ and $[K_g]$ are defined as the thermal buckling load parameters and the global geometric stiffness matrix, respectively.

2.14 Work done due to external transverse load

Using finite element model, Eq. (37) may be written as (Shegokar and Lal 2013)

$$\Pi_3 = \sum_{e=1}^{NE} \Pi_3^{(e)} = \sum_{e=1}^{NE} \{q\}^{(e)T} \{q_m\}^{(e)}$$

$$= q_m \left\{ 0 \quad \frac{l_e}{2} \quad \frac{l_e^2}{12} \quad 0 \quad 0 \quad \frac{l_e}{2} \quad -\frac{l_e^2}{2} \right\}^{T(e)} \qquad (44)$$

Where, le is the elemental length of the beam.

3. Governing equation of bending

The governing equation for the nonlinear static analysis can be derived using Variational principle, which is generalization of the principle of virtual displacement. For the bending analysis, the minimization of first variation of total potential energy Π ($\Pi_1 + \Pi_F - \Pi_2 - \Pi_3$) with respect to displacement vector is given by

$$\partial\left(\Pi_1 + \Pi_F - \Pi_2 - \Pi_3\right) = 0 \qquad (45)$$

By substituting the Eq. (40), Eq. (41), Eq. (42) and Eq. (43) and obtains as

$$\left[K\right]\{q\} = \{F\} \qquad (46)$$

With

$$\left[K\right] = \left[K_l + K_{nl} + K_{lf} + K_{nlf} - \lambda K_g\right]$$

The stiffness matrix $[K]$ consists of linear and nonlinear plate and foundation stiffness matrices and geometric stiffness matrix $[K_g]$. The parameters $\{q\}$ and $\{F\}$ are the transverse deflection and force vector respectively.
The solution of Eq. (46) can be obtained using standard solution procedure such as direct iterative, incremental and/or Newton-Raphson method etc. However, Newton Raphson method is one of the most popular and widely used
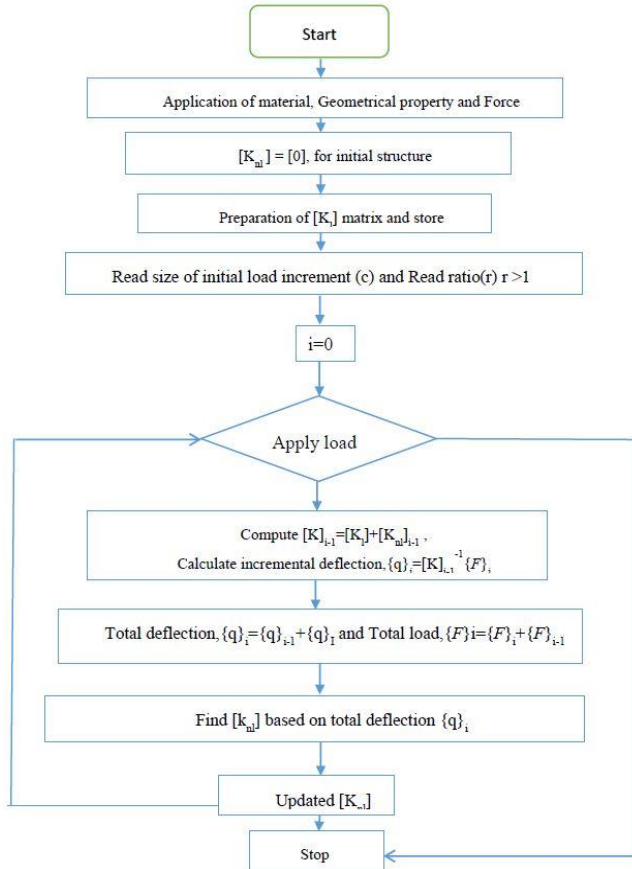
Fig. 3 Flow chart for Newton Raphson force incremental technique

solution procedure due to fast convergence at higher amplitude.

3.1 Solution approach: Newton Raphson method

The system of nonlinear static Eq. (46), can be written as (Reddy 2004)

$$\left[K(\{q\}) \right]\{q\} = \{F\} \qquad (47)$$

Where $[K(\{q\})]$ is the global nonlinear stiffness matrix, which is function of unknown global nodal displacement vector $\{q\}$ and global force vector $\{F\}$

1. The nonlinear matrix is assume as zero and evaluate the nodal displacement $\{q\}$ by taking linear stiffness matrix.

2. The nodal force vector $\{F\}$ is normalized.

3. For the specified maximum force at the center of the plate, the force vector $\{F\}$ is scaled up by C times so that resultant $\{F\}$ will have a force C at the maximum nodal force.

4. Using scaled up normalized force, the nonlinear stiffness matrix is obtained. The problem may now again have treated as static equation with new updated stiffness matrix.

5. Steps 2 to 4 are repeated by replacing by replacing $\{q\}$ linear to nonlinear $\{qnl\}$ in steps (1) and (2), to obtained converged displacement with prescribed accuracy of 10-3.

6. Repeat steps 1 to 5. For various values of C.

The detail flowchart procedure for evolution of nonlinear stiffness matrix is shown in Fig. 3.

4. Result and discussion

A user interactive computer program in MATLAB [R2015a] environment has been developed to evaluate the nonlinear transverse central deflection of multiwall nanotube (MWCNT) reinforced with conventional fiber composite elastically supported beam subjected to uniformly distributed static transverse loadings under thermal environment. The typical numerical results for different CNT volume fractions, foundation parameters, support boundary conditions aspect ratio, load parameters, temperature change, combination of ply orientations, beam aspect and thickness ratios, and variation in number of walls of CNT are presented.

The following Boundary conditions used in the present nonlinear bending analysis is,

Both edges are simply supported (SS): $u=w=0$; at $x=0$, a

Both edges are clamped (CC): $u=w=\theta x=\psi x=0$; at $x=0$, a

One edge is clamped and other is simply supported (CS): $u=w=\theta x=\psi x=0$; at $x=0$ and $u=w=0$; at $x=a$

One edge is free and other edge is clamped (FC): $u=w=\theta x=\psi x=0$; at $x=a$

One edge is free and other is simply supported (FS): $u=w=0$; at $x=a$

The following dimensionless nonlinear transverse central deflection (WO), foundation and stress parameters are used in present analysis are

$$W_O = W/h, \quad K_1 = k_1 \frac{E_m I}{a^4}, \quad K_2 = k_2 \frac{E_m I}{a^2}, \quad K_3 = k_3 \frac{E_m h}{a^4},$$

$$\sigma_{xx0} = -\frac{\sigma_{xx}(a/2, -h/2)}{q_m}, \quad \sigma_{xz0} = -\frac{\sigma_{xz}(a/2, -h/2)}{q_m} \qquad (48)$$

Where W is the dimensional transverse central deflection of CNTRC beam. The parameter I is the moment of inertia and equal to $bh^3/12$. The parameters σ_{xx} and σ_{xz} are dimensional longitudinal and transverse stress respectively.

The detailed numerical solution for the flexural analysis of MWCNTRCB subjected to uniformly distributed static loading in thermal environment for single and multi-walled carbon nanotube is presented. We first need to determine the effective material properties of MWCNTRCs. Poly (methyl methacrylate), referred to as PMMA, is selected for the matrix, and the material properties is assumed to be $E_m=(3.52-0.0034T)$GPa, $v_m=0.3$, $\rho_m=1180$ Kg/m^3. The (10, 10) SWCNTs are selected as reinforcements, whose material properties are selected as, $E_{cnt}=1.0$ TPa, $v_{cnt}=0.28$, $\rho_{cnt}=1300$ Kg/m^3. For the initial study $L_{cnt}/d_{cnt}=100$, $h_{in}=1.5\times t_{cnt}$. The material properties the E-glass fiber are taken as in the form of Young's modulus, shear modulus and Poisson ratio as $E_f=69$ GPa, $G_f=28.28$ GPa and $v_f=0.22$, respectively.

Fig. 4 shows the variation in (a) elastic modulii and (b) poisson's ratio of elastically supported single walled carbon nanotube composite beam (ESSWCNTCB) and multi walled carbon nanotube composite beam (ESMWCNTCB)
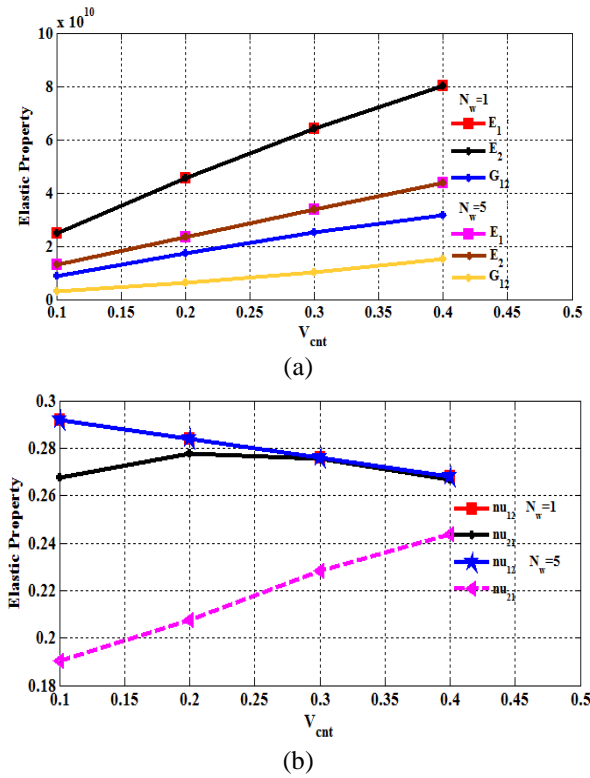
(a)

(b)

Fig. 4 Variation in mechanical properties with CNT volume fraction for (a) variation of elastic modulii and (b) poisson's ratio
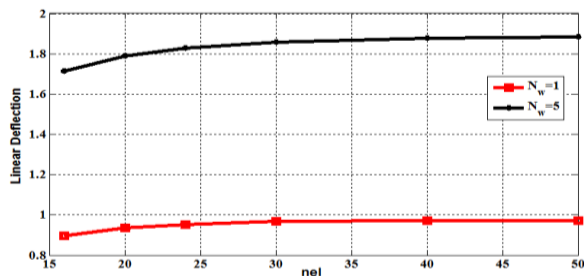

Fig. 5 Convergence study on linear deflection of MWCNTRCB with number of elements
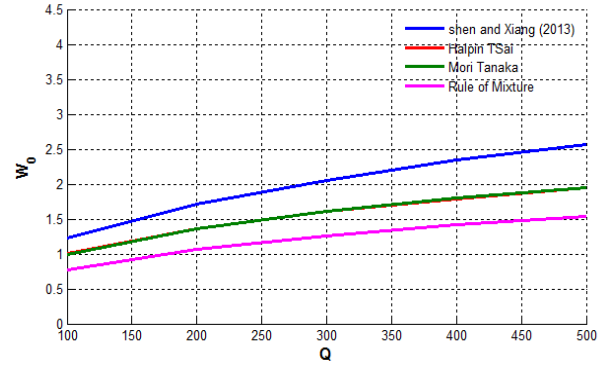

Fig. 6 Validation study of SWCNT reinforced laminated composite beam with the FG-CNTRC beams with uniformly distributed SWCNT beam
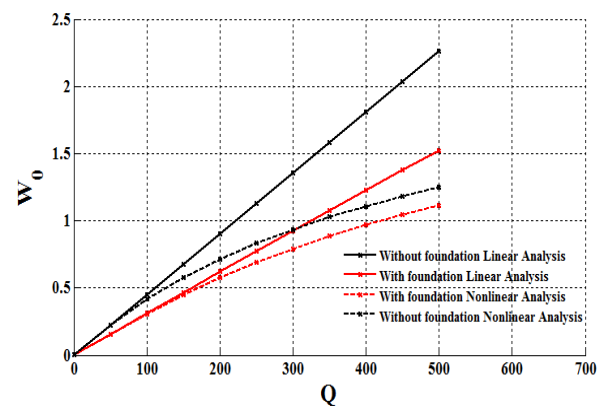

Fig. 7 Variation of transverse central deflection with load parameters for linear and non-linear analysis

Xiang 2013) using semi- analytical method. It is also found that the results obtained from the Halpin Tsai model shows very close agreement with the Mori Tanaka approach. So for the further study, the Halpin Tsai model is chosen.

4.2 Parametric study

Fig. 7 shows the effect of dimensionless linear and non-linear transverse central deflection with load factor without and with ESMWCNTCB of [0/90/0/90] under thermal environment for T=300 K and k_1=10000, k_2=100, k_3=100, V_{cnt}=0.2, simply supported. The linear transverse central deflection (NTD) follows linear nature during linear analysis while nonlinear NTD follow nonlinear nature during nonlinear analysis.

Fig. 8 shows the effect of dimensionless transverse central displacements with load factor, numbers of CNT, temperature and volume fraction of ESMWCNTCB under thermal environment for [0/90/0/90], T=300 K, V_{cnt}=0.2, k_1=10000, k_2=0, k_3=1000 and simply supported. With the increase of number of CNT and temperature change the transverse central deflection of ESMWCNTCB increases. It is because number of CNT and temperature change makes the stiffness of the beam decreases. With the increase of CNT volume fraction, the deflection of ESMWCNTCB decreases. It is because of small increase of CNT fiber volume fraction makes the beam stronger. The effect of

with SWCNT and MWCNT volume fraction variation.

4.1 Convergence and validation study

Fig. 5 shows the convergence study for the different number of elements (nel) clamped supported MWCNTRC. As nel increases, the linear deflection in the SWCNTRC and MWCNTRC beam increases and converges from nel equal to 30 and onward. Hence for the further study, total number of elements 30 are considered in the present analysis.

Fig. 6 shows the effect of foundation stiffness on the load-central deflection curves of CNTRC uniformly distributed SWCNT beam subjected to a uniformly distributed force at 300K with a/h=20, V_f=0.17. Present results using C^0 finite element method using Halpin Tsai model, Mori Tanaka method and Rule of mixture are in good agreement with the results available in (Shen and
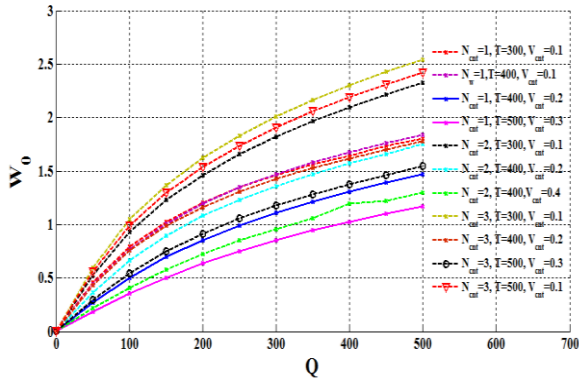
Fig. 8 Variation of transverse central deflection with load factor for different number of CNT wall, temperature and CNT volume fraction

Fig. 11 Variation of transverse central deflection with load factor for different support conditions
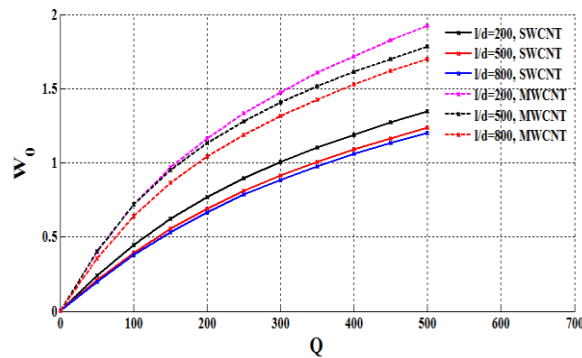

Fig. 9 Variation of transverse central deflection with load factor for different aspect ratio (l/d)

Fig. 12 Variation of transverse central deflection with load factor for different foundation parameters
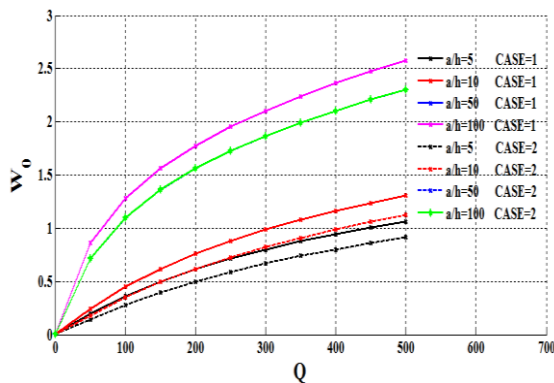

Fig. 10 Variation of transverse central deflection with load factor for different thickness ratios

change of volume fraction is highest while change of temperature is lowest.

Fig. 9 shows the effect of dimensionless transverse central displacements with load factor, length to diameter ratios of ESMWCNTCB under thermal environment for [0/90/0/90], T=300 K, V_{cnt}=0.2, k_1=10000, k_2=0, k_3=1000 and simply supported. As the aspect ratio of SWCNT or MWCNT increases the transverse central deflection of ESSWCNTCB and ESMWCNTCB lowers down. During this study aspect ratio is varied by changing the length of CNT with constant diameter. The change is more significant in SWCNT. In case of SWCNT-RC the rate of lowering the
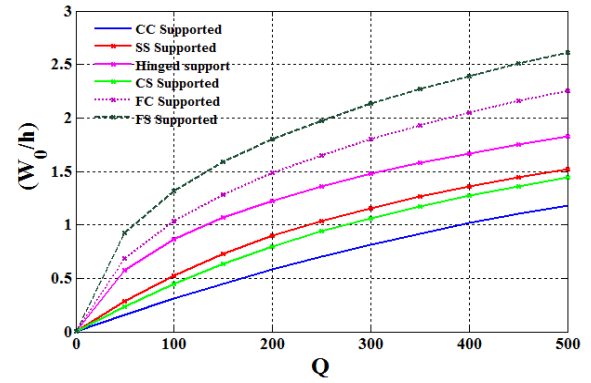
central transverse deflection is around 9.5% and 1.6%. But in case of MWCNT-RC already the deflection is more as compared to SWCNT-RC, and rate of decrement in transverse deflection is around 7% and 4.4%.

Fig. 10 shows dimensionless transverse central displacement with load factor of ESSWCNTCB and ESMWCNTCB simply supported under thermal environment for T=300 K, V_{cnt}=0.3, k_1=0, k_2=0, k_3=0 and [0/90/0/90]. In case I and 2, the width of the beam is considered as one third of length, whereas in second case width of the beam is considered as one fourth of length. It is observed that as (a/h) increases, the beam deflection also increases. A side from other, with the increase of width of the beam, the nonlinear transverse deflection decreases due to increase of transverse resistant.

Fig. 11 shows the dimensionless transverse central displacements with load factor, support conditions and changed of ESMWCNTCB under thermal environment of 300K for k_1=10000, k_2=100, k_3=100, V_{cnt}=0.2 and [0/90/0/90]. It is concluded that Among the different boundary conditions simply supported (SS), clamped supported (CS), Hinged supported (HS), Free-Clamped (FC), Free Simply supported (FS) minimum transverse central deflection is produced in clamped supported beam (CC) whereas maximum transverse central deflection is produced at Free Simply supported (FS) due to more number of boundary constraints.

Fig. 11 shows the dimensionless transverse central
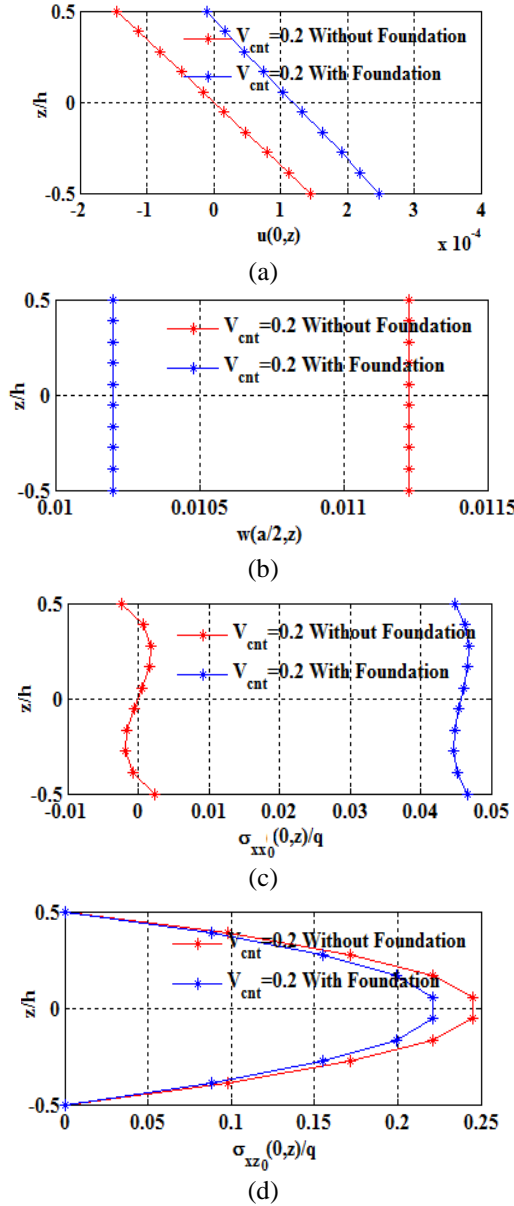
(a)

(b)

(c)

(d)

Fig. 13 Effect of (a) in plane displacement (b) transverse displacement (c) longitudinal stress and (d) shear stress through the thickness direction of with and without foundation
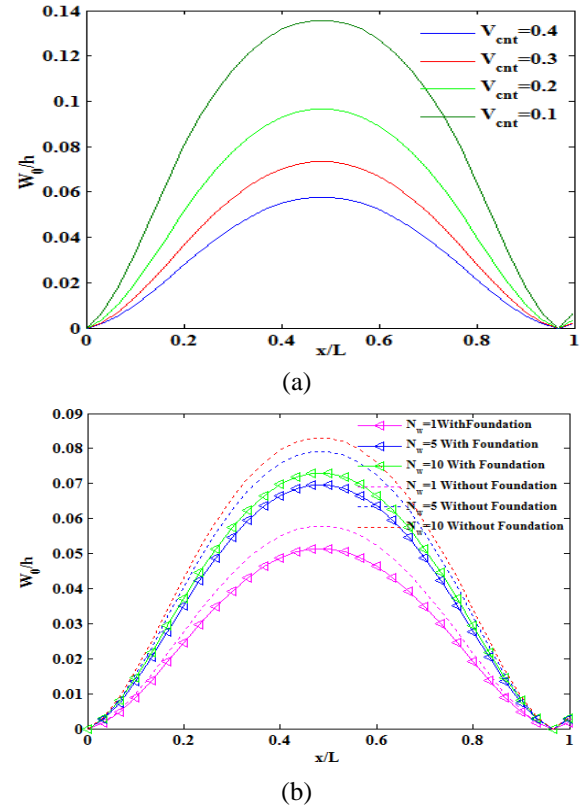

(a)

(b)

Fig. 14 Effect of transverse deflection along the length of beam for different (a) CNT volume fraction (b) number of CNT walls with elastic foundation

displacements with load factor, support conditions and changed of ESMWCNTCB under thermal environment of 300K for k_1=10000, k_2=100, k_3=100, V_{cnt}=0.2 and [0/90/0/90]. It is concluded that Among the different boundary conditions simply supported (SS), clamped supported (CS), Hinged supported (HS), Free-Clamped (FC), Free Simply supported (FS) minimum transverse central deflection is produced in clamped supported beam (CC) whereas maximum transverse central deflection is produced at Free Simply supported (FS) due to more number of boundary constraints.

Fig. 12 shows the effect of dimensionless transverse central displacements with load factor, support conditions and foundation parameters of ESMWCNTCB under thermal environment for [0/90/0/90], T=300K, V_{cnt}=0.3, and simply supported. It is concluded that among the combination of different foundation parameters, with the increase of foundation parameters, the deflection of the plate decreases due to increase the stiffness of the plate. Among the given combination of foundation parameters, effect of shear foundation parameter (k_2) is most effective and nonlinear Winkler foundation parameter is least sensitive. Hence for higher stability and safety point of view, proper modeling and design of shear foundation is extremely important.

Fig. 13(a)-(d) shows the effect of dimensionless transverse displacements (*u* and *w*) and stresses (σxx and σxz) with thickness direction (*z/h*) along longitudinal and transverse directions of without and with ESSWCNTCB of [0/90/0/90] under thermal environment for T=300 K and k_1=10000, k_2=100, k_3=100 simply supported. It is clear that out of plane deformation (*w*) shows no effect of elastic foundation and volume fraction due to independent of thickness direction. The effect of longitudinal stress is higher as compared to transverse stress. The transverse displacements and stresses are more sensitive for beam supported with elastic foundation.

Fig. 14(a) shows the effect of various CNT volume fraction on the transverse deflection of the ESSWCNTCB and ESMWCNTCB at 300K and CC boundary condition. As the volume fraction of CNT increases, the deflection in the beam reduced down and maximum transverse deflection is observed at the center of the beam. This shows that, as volume fraction of CNT increases in SWCNTRCB, it improves the beam stiffness and overall transverse central

Table 1 Effect of number of wall, aspect ratios and thickness of MWCNT on dimensionless maximum transverse deflections and stresses of ESMWCNTRCB

	L/d	h_{in}/t_{cnt}	u	w	σ_{xx}	σ_{xz}
$N_w=1$	10	0.5	0.011159	0.036964	0.67483	0.876511
	100	1.0	0.00253	0.0244601	0.29260	0.175464
	1000	1.5	0.0004732	0.01943	0.04692	0.2217
$N_w=5$	10	0.5	0.0164742	0.038249	0.8506489	0.0628549
	100	1.0	0.008849	0.030459	0.6415192	0.1122867
	1000	1.5	0.002695	0.02485	0.30354	0.173375
$N_w=10$	10	0.5	0.017459	0.04200	0.871175	0.053878
	100	1.0	0.011159	0.036964	0.67483	0.08765
	1000	1.5	0.0039788	0.026954	0.38449	0.14353

Table 2 Effect of lamination scheme on transverse central deflection of ESMWCNTRCB by using 2 phase conventional composite, 3 phase SWCNT reinforced matrix and 2 phase MWCNT CNT reinforced composite

Lamination scheme	Conventional fiber and matrix, $N=0$ 2 phase	Conventional fiber and matrix and CNT, $N=1$ 3 phase	Conventional matrix and CNT, $N=1$ 2 phase	Conventional matrix and CNT, $N=10$ 2 phase
90	1.69384462	0.53043565	1.55320159	1.6008766
0	0.8907035	0.529402438	0.987713747	1.393020
45/-45	1.40077743	0.530330119	1.32925845	1.514935702
60/-60	1.58098689	0.53048607	1.4699739	1.56560221

Table 3 Effect of lamination angles and aspect ratios and wall of CNTs on transverse central deflection of ESMWCNTRCB

Lamination scheme	l/d	$N=1$	$N=5$	$N=10$
$[0/90/90/0]_{2S}$	200	1.1753514	1.6263339	1.7687277
	500	1.0859869	1.4264819	1.5864327
$[0/90/0/90]_{2T}$	200	1.175382556	1.627575159	1.777949039
	500	1.0861478	1.4267509	1.5873774
$[45/-45/-45/45]_{2S}$	200	1.17565647	1.647349128	1.824614654
	500	1.087873224	1.430384242	1.602861967
$[45/-45/45/-45]_{2T}$	200	1.175656473	1.647349128	1.8246146539
	500	1.0878732235	1.4303842422	1.6028619672
$[30/-30/30/-30]_{2T}$	200	1.173573268	1.627137373	1.776398993
	500	1.084566409	1.425477557	1.586868903

deflection of beam reduces. Fig. 14(b) indicate the effect of single and multi-walled CNT on transverse deflection of beam, with and without foundation with CNT volume fraction of 0.4 and 300 K. It is conclude from the graph that deflection in beam with addition of SWCNT is minimum as compared to MWCNT, so SWCNTRCB is more significant, and this is because of the transverse resistance offered by the single walled CNT.

Table 1 shows the dimensionless transverse central deflection of ESMWCNTCB of [0/90/0/90] under thermal environment for T=300 K and k_1=10000, k_2=100, k_3=100 simply supported. The transverse central deflection and stresses increases as the number of walls in CNT increases. It is concluded that ESSWCNTCB show better resistance to flexural deformations and stresses in comparison to ESMWCNTCB. With the increase of L/d and hin/tcnt ratios, the flexural deformations and stresses again decreases drastically in SWCNT and MWCNT. The reason behind this is as length of the CNT increases diameter and number of walls increases, and tangential strength decreases.

Table 2 shows the effect of dimensionless transverse central displacements with load factor and lamination scheme of ESSWCNTCB and ESMWCNTCB simply supported, V_{cnt}=0.3, k_1=10000, k_2=100, k_3=100. Under the action of uniform loading, there is a maximum deflection occurs in a conventional 2-phase composite. But in conventional composite material with replacement of the fiber by SWCNT and MWCNT 2-phase composite shows minimized central transverse deflection in ESSWCNTCB and ESMWCNTCB and that decrement in the deflection is around 6% to 9% from conventional composite. The use of uniformly dispersed MWCNT and SWCNT dispersed into conventional matrix make and assuming as new matrix then reinforced with E-glass fiber as 3 phase composite gives lowest displacement (15% from conventional composite) among the all conditions, and that concluded the reason behind the use of three phase ESSWCNTCB and ESMWCNTCB in the present analysis.

Table 3 shows the effect of dimensionless transverse central displacements with load factor and lamination

scheme of ESSWCNTCB and ESMWCNTCB simply supported, V_{cnt}=0.3, k_1=10000, k_2=100, k_3=100, T=300 K. This table shows the effect of layers and l/d ratio on beam deflection. Under the action of uniform loading and thermal environment, there is a more deflection occurs in a MWCNTR composite beam. As length of CNT increases, the corresponding central transverse deflection reduced down. So the MWCNT length is the sensitive parameter in case of ESSWCNTCB and ESMWCNTCB.

5. Conclusions

In this paper, thermo-mechanically induced non-linear response of multiwall carbon nanotube reinforced laminated composite beam (MWCNTRCB) supported by elastic foundation using higher order shear deformation theory and von-Karman non-linear kinematics. The flowing observation is obtained from the limited study:

The increase of number of CNT and temperature significantly increase the central deflection. The CNT volume fraction significantly decreases the transverse central deflection. It is concluded that SWCNT with lower temperature and higher CNT volume fraction can gives better transverse strength. The increase of length and thickness of SWCNT or MWCNT significantly decrease the central deflection and stresses. It is concluded that long and straight CNT with higher thickness can gives better transverse strength. Effect for supporting elastic foundations play an important role of higher safety and stability of original structures. Hence structures should always be supported by elastic foundation with higher shear foundation stiffness. For higher transverse strength these two parameters should be high. The thickness and width of the beam decreases the transverse central deflection. The clamped supported beam shows lowest deflection while hinged support condition gives highest deflection. Higher strength of either matrix or fiber decreases the transverse deflection. Therefore, replacement of the fiber by SWCNT and MWCNT shows minimized transverse central deflection in ESSWCNTCB and ESMWCNTCB. The use of uniformly dispersed MWCNT and SWCNT into polymer matrix and then reinforced with fiber gives lowest transverse central deflection among the all conditions.

References

Bhardwaj, G., Upadhyay, A.K., Pandey, R. and Shukla, K.K. (2013), "Non-linear flexural and dynamic response of CNT reinforced laminated composite plates", *Compos.: Part B*, **45**, 89-100.

Bonnet, P., Sireude, D., Garnier, B. and Chauvet, O. (2007), "Thermal properties and percolation in carbon nanotube-polymer composites", *J. Appl. Phys.*, **91**, 2019-2030.

Capozucca, R. and Cerri, M.N. (2002), "Static and dynamic behaviour of RC beam model Strengthened by CFRP-sheets", *Constr. Build. Mater.*, **16**(2), 91-99.

Caudhari, V.K., Niranjan, L.S. and Lal, A. (2014), "Stochastic nonlinear bending response of elastically supported nanotube-reinforced composite beam in thermal environment", *Int. J. Comput. Mater. Sci. Eng.*, **6**(2), 1750020.

Chakrabortya, A., Gopalakrishnana, S. and Reddy, J.N. (2003), "A new beam finite element for the analysis of functionally graded materials", *Int. J. Mech. Sci.*, **45**, 519-539.

Colombi, P. and Poggi, C. (2005), "An experimental, analytical and numerical study of the static behaviour of steel beams reinforced by pultruded CFRP strips", *Compos.*, **37**(1), 64-73.

Deng, J. and Lee, M.M.K. (2007), "Behaviour under static loading of metallic beams reinforced with a bonded CFRP plate", *Compos. Struct.*, **78**(2), 232-242.

Fidelus, J.D., Wiesel, E., Gojny, F.H., Schulte, K. and Wagner, H.D. (2005), "Thermo-mechanical properties of randomly oriented carbon/epoxy nanocomposites", *Compos. Part A*, **36**, 1555-1561.

Han, Y. and Elliott, J. (2007), "Molecular dynamics simulations of the elastic properties of polymer/carbon nanotube composites", *Comput. Mater. Sci.*, **39**, 315-323.

Han, Y. and Elliott, J. (2007),"Molecular dynamics simulations of the elastic properties of polymer/carbon nanotube composites", *Comput. Mater. Sci.*, **39**, 315-323.

Kapania, R.K. and Raciti, S. (1989), "Recent advances in analysis of laminated beams and plates. Part I-Shear effects and buckling", *AIAA J.*, **27**(7), 923-935.

Kerur, S.B. (2013), "Geometrically nonlinear static and dynamic analysis of piezoelectric fiber reinforced composite plates and shells", IIT Kharagpur.

Kishan, K.P. and Suresh, J.K. (2017), "Bending analysis of CNT reinforced metal matrix composite rectangular plates using higher order shear deformation theory", *IJRASET*, **5**, 2231-2244.

Kumar, P. and Srinivas, J. (2017), "Free vibration, buckling and bending behavior of a FG-CNT reinforced composite beam: comparative analysis with hybrid laminated composite beam", *Multidisc. Model. Mater. Struct.*, **13**(4), 590-611.

Kumar, P. and Srinivas, J. (2017), "Vibration, buckling and bending behavior of functionally graded multi-walled carbon nanotube reinforced polymer composite plates using the layer-wise formulation", *Compos. Struct.*, **177**, 158-170.

Lal, A., Singh, B.N. and Kumar, R. (2007), "Natural frequency of laminated composite plate resting on an elastic foundation with uncertain system properties", *Struct. Eng. Mech.*, **27**(2), 199-222.

Pradhan, S.C. and Reddy, G.K. (2011), "Thermo mechanical buckling analysis of carbon nanotubes on winkler foundation using non-local elasticity theory and DTM", *Ind. Acad. Sci. Sadhana*, **36**(6), 1009-1019.

Reddy, J.N. (2004), *An Introduction to Nonlinear Finite Element Analysis*, Oxford University Press, Oxford.

Shegokar, N.L. and Lal, A. (2013), "Stochastic nonlinear bending response of piezoelectric functionally graded beam subjected to thermoelectromechanical loadings with random material properties", *Compos. Struct.*, **100**, 17-33.

Shen, H.S. (2000), "Nonlinear analysis of simply supported Reissner-Mindlin plates subjected to lateral pressure and thermal loading and resting on two-parameter elastic foundations", *Eng. Struct.*, **23**, 1481-1493.

Shen, H.S. (2009), "Nonlinear bending of functionally graded carbon nanotube reinforced composite plates in thermal environments", *Compos. Struct.*, **91**, 9-19.

Shen, H.S. (2011), "A novel technique for nonlinear analysis of beams on two-parameter elastic foundations", *Int. J. Struct. Stab. Dyn.*, **11**, 999-1014.

Shen, H.S. and Xiang, Y. (2013), "Nonlinear analysis of nanotube-reinforced composite beams resting on elastic foundations in thermal environments", *Eng. Struct.*, **56**, 698-708.

Shi, G., Lam, K.Y. and Tay, T.E. (1998), "On efficient finite element modeling of composite beams and plates using higher-order theories and an accurate composite beam element", *Compos. Struct.*, **41**, 159-165.

Sina, S.A., Navazi, H.M. and Haddadpour, H. (2009), "An

analytical method for free vibration analysis of functionally graded beams", *Mater. Des.*, **30**, 741-747.

Singh, B.N., Lal, A. and Kumar, R. (2008), "Nonlinear bending response of laminated composite plates on nonlinear elastic foundation with uncertain system properties", *Eng. Struct.*, **30**, 1101-1112.

Song, Y.S. and Youn, J.R. (2006), "Modeling of effective elastic properties for polymer based carbon nanotube", *Compos. Polym.*, **47**, 1741-1748.

Syed, S.H., Muttappa, D., Mahammadrafeeq, M. and Sunil, T. (2017), "Numerical study on static behavior of fiber reinforced composite panels", *Int. J. Mech. Prod. Eng.*, **5**(11), 15-21.

Tahouneh, V. (2017), "Using modified Halpin-Tsai approach for vibrational analysis of thick functionally graded multi-walled carbon nanotube plates", *Steel Compos. Struct.*, **23**(6), 657-668.

Tahouneh, V. (2017), "Vibration and mode shape analysis of sandwich panel with MWCNTs FG-reinforcement core", *Steel Compos. Struct.*, **25**(3), 347-360.

Tahouneh, V. (2018), "3-D Vibration analysis of FG-MWCNTs/Phenolic sandwich sectorial plates", *Steel Compos. Struct.*, **26**(5), 649-662.

Thostenson, E.T., Ren, Z. and Chou, T.W. (2001), "Advances in the science and technology of carbon nanotubes and their composites: a review", *Compos. Sci. Techno.*, **l61**(18), 1899-1912.

Vo, T.P. and Thai, H.T. (2012), "Static behaviour of composite beams using various refined shear deformation theories", *Compos. Struct.*, **94**(8), 2513-2522.

Wan, H., Delale, F. and Shen, L. (2005), "Effect of CNT length and CNT, matrix interphase in carbon nanotube (CNT) reinforced composites", *Mech. Res. Commun.*, **32**, 481-489.

William, H., Teukolsky, A.S., William, T.V. and Flannery, P.B. (1992), *Numerical Recipes in Fortran*, 2nd Edition, Cambridge University Press, Cambridge.

Wuite, J. and Adali, S. (2005), "Deflection and stress behavior of nano composites reinforced beams using a multiscale analysis", *Compos. Struct.*, **71**, 388-396.

Yas, M.H. and Heshmati, M. (2012), "Dynamic analysis of functionally graded nanocomposite beams reinforced by randomly oriented carbon nanotube under the action of moving load", *Appl. Math. Model.*, **36**, 1371-1394.

Yass, M.H. and Samadi, N. (2012), "Free vibrations and buckling analysis of carbon nanotube-reinforced composite Timoshenko beams on elastic foundation", *Int. J. Press. Ves. Pip.*, **98**, 119-128.

Ying, J., Lu, C.F. and Chen, W.Q. (2008), "Two-dimensional elasticity solutions for functionally graded beams resting on elastic foundations", *Compos. Struct.*, **84**, 209-219.

Zhang, W. and Xiao, L.N. (2017), "Mechanical behavior of laminated CNT-reinforced composite skew plates subjected to dynamic loading", *Compos. Part B*, **122**, 219-230.

Zhu, R., Pan, E. and Roy, A.K. (2007), "Molecular dynamics study of the stress-strain behavior of carbon-nanotube reinforced Epon 862 composites", *Mater. Sci. Eng. A*, **447**, 51-57.

HK

Nomenclature and Abbreviation

a, b, h	=	Length, width and thickness of beam
l, d, h_{in}, t_{cnt}	=	Length, diameter, inner wall spacing and thickness of CNT
E_f, v_f	=	Longitudinal and poison's ratio of conventional fiber
G	=	Shear modulus of conventional composite
E_m, v_m, v_m	=	Young's modulus poison's ratio and volume fraction of matrix
$E_{cnt}, v_{cnt}, V_{cnt}(=V_f)$	=	Young's modulus, poison's ratio and volume fraction of SWCNT/ MWCNT
W, W_0	=	Dimensional and dimensionless transverse central deflection
q, Q	=	Dimensional load and non-dimensional load parameter
$SWCNT$	=	Single Wall Carbon Nanotube
$SWCNTRC$	=	Single Wall Carbon Nanotube Reinforced Composite
$MWCNTRC$	=	Multi Wall Carbon Nanotube Reinforced Composite
$ESMWCNTRCB$	=	Elastically supported multiwall carbon reinforced composite beam
K_1, K_2, K_3	=	Linear normal, shear and nonlinear normal foundations stiffness
k_1, k_2, k_3	=	Linear normal, shear and nonlinear normal foundation stiffness parameters
T, T_0	=	Applied and room temperature
α_{cnt}, α_m	=	Thermal expansion coefficient of CNT and matrix
$[K_l], [K_{nl}]$	=	Global linear and nonlinear stiffness matrices